Hybrid colored noise process with space-dependent switching rates

Paul C. Bressloff and Sean D. Lawley
Department of Mathematics, University of Utah, Salt Lake City, Utah 84112, USA
(Received 23 May 2017; published 13 July 2017)

A fundamental issue in the theory of continuous stochastic process is the interpretation of multiplicative white noise, which is often referred to as the Itô-Stratonovich dilemma. From a physical perspective, this reflects the need to introduce additional constraints in order to specify the nature of the noise, whereas from a mathematical perspective it reflects an ambiguity in the formulation of stochastic differential equations (SDEs). Recently, we have identified a mechanism for obtaining an Itô SDE based on a form of temporal disorder. Motivated by switching processes in molecular biology, we considered a Brownian particle that randomly switches between two distinct conformational states with different diffusivities. In each state, the particle undergoes normal diffusion (additive noise) so there is no ambiguity in the interpretation of the noise. However, if the switching rates depend on position, then in the fast switching limit one obtains Brownian motion with a space-dependent diffusivity of the Itô form. In this paper, we extend our theory to include colored additive noise. We show that the nature of the effective multiplicative noise process obtained by taking both the white-noise limit ($\kappa \to 0$) and fast switching limit ($\epsilon \to 0$) depends on the order the two limits are taken. If the white-noise limit is taken first, then we obtain Itô, and if the fast switching limit is taken first, then we obtain Stratonovich. Moreover, the form of the effective diffusion coefficient differs in the two cases. The latter result holds even in the case of space-independent transition rates, where one obtains additive noise processes with different diffusion coefficients. Finally, we show that yet another form of multiplicative noise is obtained in the simultaneous limit $\epsilon,\kappa \to 0$ with ϵ/κ^2 fixed.

DOI: 10.1103/PhysRevE.96.012129

I. INTRODUCTION

Fundamental issues in nonequilibrium statistical physics are the interpretation of multiplicative white noise and the associated distinction between Itô and Stratonovich versions of stochastic differential equations (SDEs) [1–3]. Additional physical constraints are usually required to identify the correct interpretation. For example, taking the white-noise limit of a particle driven by colored multiplicative noise generates the Stratonovich version [4]. On the other hand, consistency of the stochastic dynamics with equilibrium statistical physics yields the so-called kinetic interpretation [5–7]. The latter appears to hold in experiments observing the motion of a colloidal particle near a wall, where hydrodynamic interactions lead to spatial variations in the diffusion coefficient D of a Brownian particle (heterogeneous diffusion) [8–10].

There has also been a recent resurgence of interest in heterogeneous diffusion within biological cells, driven by advances in single-particle tracking (SPT) experiments [11–14]. These experiments track the trajectories of individual macromolecules and lipids within the plasma membrane by attaching an observable tag such as a quantum dot, gold nanoparticle, or fluorophore. They have established that, rather than moving freely, molecules tend to exhibit heterogenous dynamics, including confined and anomalous diffusion. A variety of mechanisms have been proposed to explain such behavior, including lipid microdomains [15], compartmentalization by the cytoskeleton (the so-called picket-fence model [13]), and protein-protein interactions [16–18]. The simplest technique for analyzing SPT data is to detect deviations from free diffusion based on the mean squared displacement (MSD). It is well known that unconfined Brownian motion has a cumulative MSD that is a linear function of time, whereas a sublinear temporal variation of MSD is indicative of movement in a confined environment and a supralinear variation suggests directed motion. One can then compare various physical models by fitting theoretical MSD curves with the data. One limitation of MSD as a measure of heterogeneous diffusion is that it is based on the statistics of multiple trajectories. However, it is also possible to detect heterogeneity within single trajectories by utilizing statistics to detect deviations from generic properties of Brownian motion, including first passage times and occupation times [19–22]. Yet a more effective statistical method is to use parametric models of heterogeneous diffusion, based on the hidden Markov model (HMM) framework [23–25]. These latter studies suggest that particles within the plasma membrane can switch between different discrete conformational states with different diffusivities. Such switching could be due to interactions between proteins and the actin cytoskeleton [23] or due to protein-lipid interactions [26].

Motivated by the above experimental studies, we have recently analyzed a model of a Brownian particle that randomly switches between two distinct conformational states with different diffusivities [27]. In each state, the particle undergoes normal diffusion (additive noise) so there is no ambiguity in the interpretation of the noise. However, if the switching rates depend on position, then in the fast switching limit $\epsilon \to 0$, where ϵ is some dimensionless scale factor, one obtains Brownian motion with a space-dependent diffusivity of the Itô form. (The case of space-independent switching between two diffusive states has recently been analyzed in Ref. [28].) In this paper, we extend our theory to include colored additive noise with correlation time κ. We show that the nature of the effective multiplicative noise process obtained by taking both the white-noise limit ($\kappa \to 0$) and fast switching limit ($\epsilon \to 0$) depends on the order the two limits are taken. If the white-noise limit $\kappa \to 0$ is taken

first, then we obtain an Itô SDE, whereas a Stratonovich SDE is obtained when the fast switching limit $\epsilon \to 0$ is taken first. Moreover, the form of the effective diffusion coefficient differs in the two cases. The latter result holds even in the case of space-independent transition rates, where one obtains additive noise processes with different diffusion coefficients.

The structure of the paper is as follows. In Sec. II we formulate our model and sketch the main results of the paper. We then carry out a more detailed derivation of our results in Sec. III, where we analyze the adiabatic and white-noise limits using projection methods. We present an alternative approach in Sec. IV based on regular perturbation theory. This allows us to derive yet another form of multiplicative noise in the simultaneous limit $\epsilon,\kappa \to 0$ with ϵ/κ^2 fixed. Finally, we present some numerical results in Sec. V and conclude with a brief discussion.

II. A HYBRID COLORED NOISE PROCESS

Let $X(t) \in \mathbb{R}$ denote the position of a particle at time t, which is taken to evolve according to the stochastic differential equation (SDE)

$$dX(t) = \frac{1}{\kappa} f(X(t))Y(t)dt, \tag{2.1a}$$

where $Y(t)$ is a stochastic external input evolving according to the Ornstein-Uhlenbeck process

$$dY(t) = -\frac{\gamma}{\kappa^2}Y(t)dt + \frac{1}{\kappa}W(t),$$
$$\langle dW(t)\rangle = 0, \quad \langle dW(t)dW(t')\rangle = \delta(t-t')dtdt', \tag{2.1b}$$

where δ is the Dirac δ function. We take κ to be dimensionless so that γ is a scaled decay rate. For simplicity, we fix the units of time by setting $\gamma = 1$. Heuristically speaking, in the white-noise limit $\kappa \to 0$ we can set $Y(t)dt = \kappa dW(t)$ such that we obtain a scalar SDE of the Stratonovich form:

$$dX(t) = f(X(t)) \circ dW(t). \tag{2.2}$$

One way to establish the correct interpretation of the multiplicative noise is to start with the full two-dimensional (2D) Itô Fokker-Planck (FP) equation for the probability density function of sample paths and to reduce it to a scalar Stratonovich FP equation in the limit $\kappa \to 0$ using an adiabatic reduction and projection methods [4].

Now consider a hybrid version of the above SDE, in which the nonlinear function $f(X)$ is replaced by a piecewise constant function $\sqrt{2D_{N(t)}}$, with $N(t) \in \{0,1\}$ evolving according to a two-state Markov chain

$$0 \underset{\alpha/\epsilon}{\overset{\beta/\epsilon}{\rightleftharpoons}} 1, \tag{2.3}$$

with $\epsilon > 0$, a dimensionless parameter. That is,

$$dX(t) = \frac{1}{\kappa}\sqrt{2D_{N(t)}}Y(t)dt, \tag{2.4a}$$

$$dY(t) = -\frac{1}{\kappa^2}Y(t)dt + \frac{1}{\kappa}dW(t). \tag{2.4b}$$

for $N(t) \in \{0,1\}$ and D_0, D_1 constants. We can view this as a three-component stochastic hybrid system, $(X,Y,N) \in \mathbb{R} \times \mathbb{R} \times \{0,1\}$. Following Ref. [27], we will assume that the switching rates α,β depend on the current position of the particle, $\alpha = \alpha(X(t))$, $\beta = \beta(X(t))$.

Suppose that it is still possible to take the white-noise limit for the nonautonomous SDE (2.4). For fixed $\epsilon > 0$, we would then obtain the following piecewise SDE for the position $X(t)$:

$$dX(t) = \sqrt{2D_{N(t)}}\, dW(t). \tag{2.5}$$

As it stands, the resulting additive SDE represents a Brownian particle with a switching diffusion coefficient and space-dependent switching rates. This stochastic hybrid system was analyzed in Ref. [27], where we showed that taking $\epsilon \to 0$ yields an Itô equation for $X(t)$,

$$dX(t) = \sqrt{2\overline{D}(X(t))}\, dW(t), \tag{2.6}$$

where

$$\overline{D}(x) = \sum_{n=0,1} \rho_n(x) D_n \tag{2.7}$$

and

$$\rho_0(x) = \frac{\alpha(x)}{\alpha(x)+\beta(x)}, \quad \rho_1(x) = 1 - \rho_0(x). \tag{2.8}$$

For fixed x, $\rho_n(x)$, $n = 0,1$ corresponds to the unique stationary distribution of the two-state Markov chain with generator $\epsilon^{-1}\mathbf{A}(x)$, where

$$\mathbf{A}(x) = \begin{pmatrix} -\beta(x) & \alpha(x) \\ \beta(x) & -\alpha(x) \end{pmatrix}. \tag{2.9}$$

In particular, $\sum_{m=0,1} A_{nm}(x)\rho_m(x) = 0$ for $n = 0,1$. The basic intuition behind Eq. (2.6) is that in the fast switching limit $\epsilon \to 0$, the Markov chain undergoes many jumps over a small time interval Δt during which $\Delta X \approx 0$, and thus the relative frequency of the two discrete states n is approximately $\rho_n(x)$.

An alternative limit is obtained if we fix $\kappa > 0$ and perform the adiabatic limit $\epsilon \to 0$. Using similar arguments to Ref. [27], we expect that the system reduces to an effective SDE for $[X(t),Y(t)]$ of the form

$$dX(t) = \frac{1}{\kappa}\sqrt{2\widehat{D}[X(t)]}Y(t)\, dt, \tag{2.10a}$$

$$dY(t) = -\frac{1}{\kappa^2}Y(t)dt + \frac{1}{\kappa}dW(t), \tag{2.10b}$$

where

$$\widehat{D}(X) = \left[\sum_{n=0,1}\sqrt{D_n}\rho_n(x)\right]^2. \tag{2.11}$$

This would then yield an equation of the form (2.1), so taking $\kappa \to 0$ would lead to the following Stratonovich equation for X:

$$dX(t) = \sqrt{2\widehat{D}[X(t)]} \circ dW(t). \tag{2.12}$$

The above analysis suggests that the order in which the adiabatic and white-noise limits are taken has a nontrivial effect on the nature of the resulting scalar SDE for the position $X(t)$. Taking the white-noise limit first generates the Itô SDE

(2.6) with the effective diffusion coefficient $\overline{D}(x)$, whereas taking the adiabatic limit first produces a Stratonovich SDE with the effective diffusion coefficient $\widehat{D}(x)$. Interestingly, we find a difference even when the transition rates are x independent, in which case Eqs. (2.6) and (2.12) reduce to additive noise processes with different diffusion coefficients, namely, $\overline{D} = \sum_n D_n \rho_n$ and $\widehat{D}_n = (\sum_n \sqrt{D_n}\rho_n)^2$. In Sec. III we establish these results more systematically using projection and perturbation methods, and then explore a case where ϵ and κ are related in Sec. IV.

III. ANALYSIS OF ADIABATIC AND WHITE-NOISE LIMITS USING PROJECTION METHODS

The first step is to write down the full Chapman-Kolmorogov (CK) equation for the stochastic hybrid system $[X(t),Y(t),N(t)]$. Let

$$p_n(x,y,t) = \mathbb{P}[x < X(t) < x+dx, \quad y < Y(t) < y+dy, \\ N(t) = n | X_0, Y_0, n_0],$$

for fixed initial conditions. Then

$$\frac{\partial p_n(x,y,t)}{\partial t} = \frac{1}{\kappa^2}\left(\frac{\partial}{\partial y}y + \frac{1}{2}\frac{\partial^2}{\partial y^2}\right)p_n(x,y,t) \\ - \frac{\sqrt{2D_n}y}{\kappa}\left[\frac{\partial}{\partial x}\right]p_n(x,y,t) \\ + \frac{1}{\epsilon}\sum_{m=0,1} A_{nm}(x)p_m(x,y,t). \tag{3.1}$$

It is useful to rewrite Eq. (3.1) in the more compact form

$$\frac{\partial \mathbf{p}(x,y,t)}{\partial t} = \left(\left[\frac{1}{\kappa^2}\mathbb{L}_1\mathbf{I} + \frac{1}{\kappa}\mathbb{L}_2\mathbf{J}\right] + \frac{1}{\epsilon}\mathbf{A}(x)\right)\mathbf{p}(x,y,t). \tag{3.2}$$

where $\mathbf{p} = (p_0,p_1)^\top$, $\mathbf{I}$ is the 2×2 unit matrix, $\mathbf{J} = \mathrm{diag}(\sqrt{2D_0},\sqrt{2D_1})$, and

$$\mathbb{L}_1 = \frac{\partial}{\partial y}y + \frac{1}{2}\frac{\partial^2}{\partial y^2}, \quad \mathbb{L}_2 = -y\frac{\partial}{\partial x}. \tag{3.3}$$

Introduce the projection operator $\mathcal{P}$ acting on a scalar function $p(x,y)$ according to [4,29]

$$(\mathcal{P}p)(x,y) = p_s(y)\int_{-\infty}^{\infty} p(x,y')dy', \tag{3.4}$$

where $p_s(y)$ is the stationary probability density of the stochastic process $Y(t)$: $\mathbb{L}_1 p_s(y) = 0$, that is,

$$p_s(y) = \sqrt{\frac{1}{\pi}}e^{-y^2}. \tag{3.5}$$

We will assume that $\mathcal{P}$ acts on vector fields component-wise. The projection operator satisfies the following identities [4]: (i) $\mathcal{P}^2 = \mathcal{P}$; (ii) $\mathcal{P}\mathbb{L}_1 = \mathbb{L}_1\mathcal{P} = 0$; (iii) $\mathbf{A}\mathcal{P} = \mathcal{P}\mathbf{A}$; (iv) $\mathcal{P}\mathbb{L}_2\mathcal{P} = 0$; and (v) $\mathcal{P} = \lim_{t\to\infty} e^{t\mathbb{L}_1}$. The first three properties are trivial to show, and property (v) is simply a statement that $e^{\mathbb{L}_1 t}p(x,y)$ is a (non-normalized) solution to the FP equation $\partial_t p = \mathbb{L}_1 p$, which approaches the stationary density in the large-t limit. Finally, property (iv) is a consequence of the fact that

$$(\mathcal{P}\mathbb{L}_2\mathcal{P})p(x,y) = p_s(y)\int_{-\infty}^{\infty}\left[-y'\frac{\partial}{\partial x}p_s(y')dy'\right] \\ \times \int_{-\infty}^{\infty} p(x,y'')dy'' \\ \sim p_s(y)\langle y'\rangle_s \frac{\partial}{\partial x}\int_{-\infty}^{\infty} p(x,y'')dy'' = 0,$$

since $\langle y'\rangle_s = 0$.

The next step is to Laplace transform the CK equation with respect to time t:

$$s\widetilde{\mathbf{p}}(s) - \mathbf{p}(0) = \left(\left[\frac{1}{\kappa^2}\mathbb{L}_1\mathbf{I} + \frac{1}{\kappa}\mathbb{L}_2\mathbf{J}\right] + \frac{1}{\epsilon}\mathbf{A}\right)\widetilde{\mathbf{p}}(s), \tag{3.6}$$

where we have dropped the explicit dependence on x,y. We will assume the initial condition

$$p_n(x,y,0) = \rho_n(x)p_s(y)\delta(x-x_0).$$

Applying the projection operator $\mathcal{P}$ to Eq. (3.6) and using properties (ii) and (iii) yields

$$s\mathbf{V}(s) = \frac{1}{\kappa}\mathcal{P}\mathbb{L}_2\mathbf{J}\mathbf{W}(s) + \mathcal{P}\mathbf{p}(0) + \frac{1}{\epsilon}\mathbf{A}\mathbf{V}(s), \tag{3.7}$$

where

$$\mathbf{V}(s) = \mathcal{P}\widetilde{\mathbf{p}}(s), \quad \mathbf{W}(s) = (1-\mathcal{P})\widetilde{\mathbf{p}}(s).$$

Similarly, applying the projection operator $1-\mathcal{P}$ yields

$$s\mathbf{W}(s) = \left(\frac{1}{\kappa^2}\mathbb{L}_1\mathbf{I} + \frac{1}{\kappa}(1-\mathcal{P})\mathbb{L}_2\mathbf{J}\right)\mathbf{W}(s) + \frac{1}{\kappa}\mathbb{L}_2\mathbf{J}\mathbf{V}(s) \\ + (1-\mathcal{P})\mathbf{p}(0) + \frac{1}{\epsilon}\mathbf{A}\mathbf{W}(s). \tag{3.8}$$

Note that $\mathcal{P}\mathbf{p}(0) = \mathbf{p}(0)$ so that $(1-\mathcal{P})\mathbf{p}(0) = 0$.

Equations (3.1), (3.7), and (3.8) are the starting point for analyzing the double limit $\epsilon,\kappa \to 0$. We proceed by carrying out a double perturbation expansion in ϵ,κ, under the simplifying assumptions that either $\epsilon/\kappa^2 \gg 1$ (white-noise limit followed by adiabatic limit) or $\epsilon/\kappa^2 \ll 1$ (adiabatic limit followed by white-noise limit). In the former case, we invert Eq. (3.8) by carrying out a perturbation expansion in κ for fixed ϵ, substitute the resulting expression of $\mathbf{W}(s)$ in terms of $\mathbf{V}(s)$ into Eq. (3.7), and then take the limit $\kappa \to 0$. We then solve for $\mathbf{V}(s)$ by carrying out a perturbation expansion in ε. In the latter case, the roles of ϵ and κ are reversed. An alternative approach based on the backward CK equation is presented in Sec. IV, which considers a single perturbation expansion in κ with $\eta = \epsilon/\kappa^2$ fixed. The results of this section are then recovered by taking either $\eta \to \infty$ or $\eta \to 0$. Note, however, that the forward method presented here provides a basis for a more general double perturbation expansion.

A. Taking the white-noise limit ($\kappa \to 0$) first

First suppose we fix $\epsilon > 0$ and take the limit $\kappa \to 0$. We can formally invert Eq. (3.8) to obtain

$$\mathbf{W}(s) = -\frac{1}{\kappa}\Sigma(s)\mathbb{L}_2\mathbf{J}\mathbf{V}(s), \tag{3.9}$$

with

$$\Sigma(s) = \left(-s + \frac{1}{\kappa^2}\mathbb{L}_1\mathbf{I} + \frac{1}{\kappa}(1-\mathcal{P})\mathbb{L}_2\mathbf{J} + \frac{1}{\epsilon}\mathbf{A}\right)^{-1}. \quad (3.10)$$

Substituting into Eq. (3.7) thus gives

$$s\mathbf{V}(s) - \mathbf{p}(0) = -\frac{1}{\kappa^2}\mathcal{P}\mathbb{L}_2\mathbf{J}\Sigma(s)\mathbb{L}_2\mathbf{J}\mathbf{V}(s) + \frac{1}{\epsilon}\mathbf{A}\mathbf{V}(s). \quad (3.11)$$

In the limit $\kappa \to 0$, we have $\Sigma(s) \to \kappa^2\mathbb{L}_1^{-1}\mathbf{I}$, so that Eq. (3.11) becomes

$$s\mathbf{V}(s) - \mathbf{p}(0) = -\mathcal{P}\mathbb{L}_2\mathbb{L}_1^{-1}\mathbb{L}_2\mathbf{J}^2\mathbf{V}(s) + \frac{1}{\epsilon}\mathbf{A}\mathbf{V}(s). \quad (3.12)$$

Now performing the inverse transform and setting

$$\lim_{\kappa\to 0} V_n(x,y,t) = p_s(y)p_n(x,t), \quad (3.13)$$

we have

$$p_s(y)\frac{\partial p_n}{\partial t} = -2D_n\left(\mathcal{P}\mathbb{L}_2\mathbb{L}_1^{-1}\mathbb{L}_2\right)p_s(y)p_n(x,t) + \frac{p_s(y)}{\epsilon}\sum_{m=0,1} A_{nm}(x)p_m(x,t). \quad (3.14)$$

It remains to calculate the second operator term on the right-hand side. From the definition of $\mathbb{L}_2$ we have

$$\begin{aligned}&\mathcal{P}\mathbb{L}_2\mathbb{L}_1^{-1}\mathbb{L}_2 p_s(y)p_n(x,t)\\ &= p_s(y)\int_{-\infty}^{\infty}\left(-\frac{\partial}{\partial x}y'\right)\mathbb{L}_1^{-1}\left(-\frac{\partial}{\partial x}y'\right)p_s(y')p_n(x,t)dy'\\ &= -\mathcal{D}p_s(y)\frac{\partial^2}{\partial x^2}p_n(x,t), \end{aligned} \quad (3.15)$$

with

$$\mathcal{D} = -\int_{-\infty}^{\infty} y\mathbb{L}_1^{-1}yp_s(y)dy. \quad (3.16)$$

Formally speaking, we have

$$\int_0^{\infty} e^{\mathbb{L}_1 t}dt = \mathbb{L}_1^{-1}(\lim_{t\to\infty} e^{\mathbb{L}_1 t} - 1) = -\mathbb{L}_1^{-1}(1-\mathcal{P}),$$

from property (v) of the projection operator. Since

$$\mathcal{P}yp_s(y) = p_s(y)\langle y\rangle_s = 0,$$

we see that

$$\mathcal{D} = \int_0^{\infty} dt\int_{-\infty}^{\infty} dy\, y[e^{\mathbb{L}_1 t}yp_s(y)].$$

Using the fact that $e^{\mathbb{L}_1 t}$ is the evolution operator of the FP equation for y, we have

$$\begin{aligned}\mathcal{D} &= \int_0^{\infty} dt\int_{-\infty}^{\infty} dy\int_{-\infty}^{\infty} dy'\, yy'p(y',t|y,0)p_s(y)\\ &= \int_0^{\infty}\langle Y(t)Y(0)\rangle_s dt = \frac{1}{2}.\end{aligned}$$

Finally, setting $\mathcal{D} = 1/2$ in Eq. (3.14), and canceling a common factor of $p_s(y)$, we arrive at the following CK equation for the probability density $p_n(x,t)$:

$$\frac{\partial p_n(x,t)}{\partial t} = D_n\frac{\partial^2 p_n(x,t)}{\partial x^2} + \frac{1}{\epsilon}\sum_{m=0,1} A_{nm}(x)p_m(x,t), \quad (3.17)$$

This is precisely the CK equation that would be written down for the joint Markov process $[N(t),X(t)]$ evolving according to the piecewise SDE (2.5).

We can now derive the Itô SDE (2.6) by carrying out a quasisteady state (QSS) or adiabatic reduction of the CK equation (3.17). This reduces the CK equation (3.17) to a corresponding FP equation for the total probability density $p(x,t) = \sum_{n=0,1} p_n(x,t)$ [4,30,31]. That is, we decompose the probability density p_n as

$$p_n(x,t) = p(x,t)\rho_n(x) + \epsilon w_n(x,t),$$

where $\sum_n w_n(x,t) = 0$. Substituting this decomposition into Eq. (3.17), summing both sides with respect to n, and using $\sum_n A_{nm}(x) = 0$ yields to leading order the Itô FP equation

$$\frac{\partial p}{\partial t} = \frac{\partial^2\overline{D}(x)p}{\partial x^2}. \quad (3.18)$$

The higher-order corrections are calculated in Ref. [27].

B. Taking the adiabatic limit ($\epsilon \to 0$) first

Next we fix $\kappa > 0$ and take the limit $\epsilon \to 0$. In this case, we cannot simply invert Eq. (3.8), since $\Sigma(s) \to \epsilon\mathbf{A}^{-1}$ as $\epsilon \to 0$, and $\mathbf{A}^{-1}$ does not exist. Instead, we introduce the decomposition

$$p_n(x,y,t) = \rho_n(x)p(x,y,t) + \epsilon w_n(x,y,t;\epsilon), \quad (3.19)$$

with $\rho_n(x)$ given by Eq. (2.8), $p(x,y,t) = \sum_{n=0,1} p_n(x,y,t)$, and $\sum_{n=0,1} w_n = 0$. Substituting into Eq. (3.1), summing both sides with respect to n, and using $\sum_n A_{nm}(x) = 0$ yields the following equation for p in the limit $\epsilon \to 0$:

$$\frac{\partial p(x,y,t)}{\partial t} = \frac{1}{\kappa^2}\left(\frac{\partial}{\partial y}y + \frac{1}{2}\frac{\partial^2}{\partial y^2}\right)p(x,y,t) - \frac{y}{\kappa}\left[\frac{\partial}{\partial x}\right]\sqrt{2\widehat{D}(x)}p(x,y,t). \quad (3.20)$$

This is precisely the two-variable FP equation for the SDE (2.10). One could now apply the projection method of Sec. III A to derive equations for $V(x,y,s) = \mathcal{P}\widetilde{p}(x,y,s)$ and $W(x,y,s) = (1-\mathcal{P})\widetilde{p}(x,y,s)$. However, a more direct method is to introduce the decompositions

$$V_n(x,y,s) = \rho_n(x)V(x,y,s) + \epsilon\nu_n(x,y,s;\epsilon), \quad (3.21a)$$

$$W_n(x,y,s) = \rho_n(x)W(x,y,s) + \epsilon\omega_n(x,y,s;\epsilon), \quad (3.21b)$$

with $\sum_n \omega_n = 0 = \sum_n \nu_n$. Substituting into Eqs. (3.7) and (3.8), summing both sides with respect to the vector components $n = 0,1$, and using $\sum_n A_{nm}(x) = 0$ then yields the following equations for V,W in the limit $\epsilon \to 0$:

$$sV(x,y,s) = \frac{1}{\kappa}\mathcal{P}\mathbb{L}_2\sqrt{2\widehat{D}(x)}W(x,y,s) + p(x,y,0)$$

and

$$sW(x,y,s) = \left[\frac{1}{\kappa^2}\mathbb{L}_1 + \frac{1}{\kappa}(1-\mathcal{P})\mathbb{L}_2\sqrt{2\widehat{D}(x)}\right]W(x,y,s) + \frac{1}{\kappa}\mathbb{L}_2\sqrt{2\widehat{D}(x)}V(x,y,s). \quad (3.22)$$

Inverting Eq. (3.22) and substituting into Eq. (3.22) gives

$$sV(x,y,s) - p(x,y,0) = -\frac{1}{\kappa}\Lambda(s)\mathbb{L}_2\sqrt{2\widehat{D}(x)}V(x,y,s),$$

where

$$\Lambda(s) = \left[-s + \frac{1}{\kappa^2}\mathbb{L}_1 + \frac{1}{\kappa}(1-\mathcal{P})\mathbb{L}_2\sqrt{2\widehat{D}(x)}\right]^{-1}.$$

Taking the limit $\kappa \to 0$ proceeds along similar lines to the analysis of Eq. (3.11). That is, taking $\Lambda(s) \to \kappa^2\mathbb{L}_1^{-1}$ and performing the inverse Laplace transform with

$$\lim_{\kappa\to 0} V(x,y,t) = p_s(y)p(x,t) \tag{3.23}$$

gives

$$p_s(y)\frac{\partial p}{\partial t} = -\left[\mathcal{P}\mathbb{L}_2\sqrt{2\widehat{D}(x)}\mathbb{L}_1^{-1}\mathbb{L}_2\sqrt{2\widehat{D}(x)}\right]p_s(y)p(x,t).$$

Evaluating the right-hand side along identical lines to the previous case and canceling a common factor of $p_s(y)$ yields the Stratonovich FP equation

$$\frac{\partial p}{\partial t} = \frac{\partial}{\partial x}\sqrt{\widehat{D}(x)}\frac{\partial}{\partial x}\sqrt{\widehat{D}(x)}p(x,t). \tag{3.24}$$

This corresponds to the Stratonovich SDE (2.12).

IV. ANALYSIS OF ADIABATIC AND WHITE-NOISE LIMITS USING THE BACKWARD EQUATION

So far we have used projection and perturbation methods to investigate how the effective forward FP equation depends on the order in which we take the adiabatic and white noise limits. To gain further insights into this issue, we develop an alternative approach in which we set $\epsilon = \kappa^2/\eta$ for some $\eta > 0$ and carry out a regular single perturbation expansion in κ. Cases A and B are then recovered in the limits $\eta \to 0$ (κ approaches zero faster than ϵ) and $\eta \to \infty$ (ϵ approaches zero faster than κ). However, for finite η we obtain yet another limit, $\epsilon,\kappa \to 0$ with ϵ/κ^2 fixed. (One could also obtain this limit using the forward method, but the analysis is more complicated.)

Adapting methods in Ref. [32], our starting point is the Kolmogorov backward equation for the three-component process $[X(t),Y(t),N(t)]$ defined in (2.3) and (2.4), which is

$$\frac{\partial}{\partial t}\mathbf{q} = \left(\frac{1}{\kappa^2}\mathbb{L}_1^* + \frac{1}{\kappa}\mathbb{L}_2^*\mathbf{J} + \frac{1}{\epsilon}\mathbf{A}^*\right)\mathbf{q}, \tag{4.1}$$

where $\mathbb{L}_1^*$ and $\mathbb{L}_2^*$ are the adjoints of (3.3),

$$\mathbb{L}_1^* = -y\frac{\partial}{\partial y} + \frac{1}{2}\frac{\partial^2}{\partial y^2}, \quad \mathbb{L}_2^* = y\frac{\partial}{\partial x},$$

$\mathbf{A}^*$ is the adjoint (transpose) of (2.9), and

$$\mathbf{q} = \begin{pmatrix} q_0(x,y,t) \\ q_1(x,y,t) \end{pmatrix}.$$

Setting $\epsilon = \kappa^2/\eta$ for some $\eta > 0$ and plugging the following power series expansion,

$$\mathbf{q} = \mathbf{q}^{(0)} + \kappa\mathbf{q}^{(1)} + \kappa^2\mathbf{q}^{(2)} + \cdots$$

into (4.1) yields the following hierarchy of equations:

$$-(\mathbb{L}_1^* + \eta\mathbf{A}^*)\mathbf{q}^{(0)} = 0, \tag{4.2}$$

$$-(\mathbb{L}_1^* + \eta\mathbf{A}^*)\mathbf{q}^{(1)} = \mathbb{L}_2^*\mathbf{J}\mathbf{q}^{(0)}, \tag{4.3}$$

$$-(\mathbb{L}_1^* + \eta\mathbf{A}^*)\mathbf{q}^{(2)} = \mathbb{L}_2^*\mathbf{J}\mathbf{q}^{(1)} - \frac{\partial}{\partial t}\mathbf{q}^{(0)} \equiv \mathbf{h}^{(2)}. \tag{4.4}$$

Ergodicity of $Y(t)$ and $N(t)$ implies that the null space of $\mathbb{L}_1^* + \eta\mathbf{A}^*$ (vectors $\mathbf{q}^{(0)}(x,y)$ for which $(\mathbb{L}_1^* + \eta\mathbf{A}^*)\mathbf{q}^{(0)} = 0$) consists of functions of the form

$$\begin{pmatrix} q_0^{(0)}(x,y,t) \\ q_1^{(0)}(x,y,t) \end{pmatrix} = \begin{pmatrix} q(x,t) \\ q(x,t) \end{pmatrix}$$

for some function $q(x,t)$. Hence, Eq. (4.3) becomes

$$-(\mathbb{L}_1^* + \eta\mathbf{A}^*)\mathbf{q}^{(1)} = y\frac{\partial}{\partial x}q(x,t)\begin{pmatrix}\sqrt{2D_0} \\ \sqrt{2D_1}\end{pmatrix} \equiv \mathbf{h}^{(1)}. \tag{4.5}$$

Now observe that the null space of $\mathbb{L}_1 + \eta\mathbf{A}$ (vectors $\mathbf{e}(x,y)$ for which $(\mathbb{L}_1 + \eta\mathbf{A})\mathbf{e} = 0$) is spanned by

$$\mathbf{e}(x,y) = p_s(y)\begin{pmatrix}\rho_0(x) \\ \rho_1(x)\end{pmatrix},$$

where $p_s(y)$ is the stationary probability density of $Y(t)$ given in (3.5). Therefore, the right-hand side of (4.5) is orthogonal to the null space of $\mathbb{L}_1 + \eta\mathbf{A}$ since

$$\begin{aligned}\langle \mathbf{h}^{(1)}, \mathbf{e}\rangle &\equiv \int_{-\infty}^{\infty}\int_{-\infty}^{\infty}\sum_{n=0,1} h_n^{(1)}(x,y)e_n(x,y)dx\,dy \\ &= \sqrt{2\widehat{D}(x)}\frac{\partial}{\partial x}q(x,t)\int_{-\infty}^{\infty} y p_s(y)\,dy = 0.\end{aligned}$$

Hence, the Fredholm alternative [33] ensures that (4.5) is solvable. Indeed, it is straightforward to check that

$$\begin{pmatrix} q_0^{(1)}(x,y,t) \\ q_1^{(1)}(x,y,t) \end{pmatrix} := \sqrt{2}\begin{pmatrix} b_0(x) \\ b_1(x)\end{pmatrix} y\frac{\partial}{\partial x}q(x,t) \tag{4.6}$$

solves Eq. (4.5), where

$$b_n(x) := \nu_\eta(x)\sqrt{\widehat{D}(x)} + [1-\nu_\eta(x)]\sqrt{D_n} \tag{4.7}$$

and

$$\nu_\eta(x) := \frac{\eta[\alpha(x)+\beta(x)]}{1+\eta[\alpha(x)+\beta(x)]}. \tag{4.8}$$

Again appealing to the Fredholm alternative, in order for Eq. (4.4) to be solvable, we need $\mathbb{L}_2^*\mathbf{J}\mathbf{q}^{(1)} - \frac{\partial}{\partial t}\mathbf{q}^{(0)}$ to be orthogonal to the null space of $\mathbb{L}_1 + \eta\mathbf{A}$. That is, we need

$$\begin{aligned}&\rho_0(x)\int_{-\infty}^{\infty} p_s(y)\left\{\mathbb{L}_2^*\sqrt{2D_0}q_0^{(1)} - \frac{\partial q}{\partial t}\right\}dy \\ &+ \rho_1(x)\int_{-\infty}^{\infty} p_s(y)\left\{\mathbb{L}_2^*\sqrt{2D_1}q_1^{(1)} - \frac{\partial q}{\partial t}\right\}dy = 0.\end{aligned}$$

Now, it is immediate that

$$\rho_0(x)\int_{-\infty}^{\infty} p_s(y)\frac{\partial q}{\partial t}\,dy + \rho_1(x)\int_{-\infty}^{\infty} p_s(y)\frac{\partial q}{\partial t}\,dy = \frac{\partial q}{\partial t},$$

since $\rho_0(x)+\rho_1(x)=\int_{-\infty}^{\infty}p_s(y)\,dy=1$ and q is independent of y. Furthermore, using (4.6) we have that

$$\begin{aligned}&\rho_n(x)\int_{-\infty}^{\infty}p_s(y)\mathbb{L}_2^*\sqrt{2D_n}q_n^{(1)}\,dy\\&=2\sqrt{D_n}\rho_n(x)\left[\int_{-\infty}^{\infty}y^2p_s(y)\,dy\right]\frac{\partial}{\partial x}\left[b_n(x)\frac{\partial}{\partial x}q(x,t)\right]\\&=\sqrt{D_n}\rho_n(x)\frac{\partial}{\partial x}\left[b_n(x)\frac{\partial}{\partial x}q(x,t)\right],\end{aligned}$$

for $n\in\{0,1\}$ since $\int_{-\infty}^{\infty}y^2p_s(y)\,dy=1/2$.

Putting this together yields the limiting backward Kolmogorov equation,

$$\frac{\partial q}{\partial t}=\sum_{n=0,1}\sqrt{D_n}\rho_n(x)\frac{\partial}{\partial x}\left[b_n(x)\frac{\partial}{\partial x}q(x,t)\right].$$

Using (4.7), this becomes

$$\begin{aligned}\frac{\partial q}{\partial t}&=\sqrt{\nu_\eta(x)\widehat{D}(x)}\frac{\partial}{\partial x}\sqrt{\nu_\eta(x)\widehat{D}(x)}\frac{\partial q}{\partial x}\\&\quad+[1-\nu_\eta(x)]\overline{D}(x)\frac{\partial^2 q}{\partial x^2}+V_\eta(x)\frac{\partial q}{\partial x},\end{aligned}$$

where

$$V_\eta(x):=\nu_\eta'(x)\left[\tfrac{1}{2}\widehat{D}(x)-\overline{D}(x)\right].$$

Therefore, the limiting SDE is

$$\begin{aligned}&dX(t)\\&=\left\{V_\eta[X(t)]+\tfrac{1}{2}\nu_\eta[X(t)]\widehat{D}'[X(t)]\right\}dt\\&\quad\times\sqrt{2\nu_\eta[X(t)]\widehat{D}[X(t)]+2\{1-\nu_\eta[X(t)]\}\overline{D}[X(t)]}\,dW(t),\end{aligned}\tag{4.9}$$

and the corresponding limiting FP equation is

$$\begin{aligned}\frac{\partial p}{\partial t}&=\frac{\partial}{\partial x}\sqrt{\nu_\eta(x)\widehat{D}(x)}\frac{\partial}{\partial x}\sqrt{\nu_\eta(x)\widehat{D}(x)}p\\&\quad+\frac{\partial^2}{\partial x^2}\{[1-\nu_\eta(x)]\overline{D}(x)p\}-\frac{\partial}{\partial x}[V_\eta(x)p].\end{aligned}\tag{4.10}$$

There are several things to note about (4.10). First, if $\kappa^2/\epsilon=\eta\to\infty$, then $\nu_\eta(x)\to 1$ and $\nu_\eta'(x)\to 0$, and we obtain the Stratonovich FP equation (3.24) corresponding to the Stratonovich SDE (2.12) with diffusion coefficient $\widehat{D}$. In the opposite limit, if $\kappa^2/\epsilon=\eta\to 0$, then $\nu_\eta(x)\to 0$ and $\nu_\eta'(x)\to 0$ and we obtain the Itô FP equation (3.18) corresponding to the Itô SDE (2.6) with diffusion coefficient $\overline{D}$. Finally, if η is finite and nonzero, then (4.10) is a mixture of Stratonovich and Itô terms plus a drift depending on the difference between $\widehat{D}$ and $\overline{D}$.

V. NUMERICAL RESULTS

In this section, we use numerical simulation to demonstrate the convergence of (2.4) to either (2.6), (2.12), or (4.9), depending on how we take the double limit $\epsilon,\kappa\to 0$. We present the numerical results first and then describe our algorithm for generating statistically exact simulations of the hybrid colored noise process (2.4).

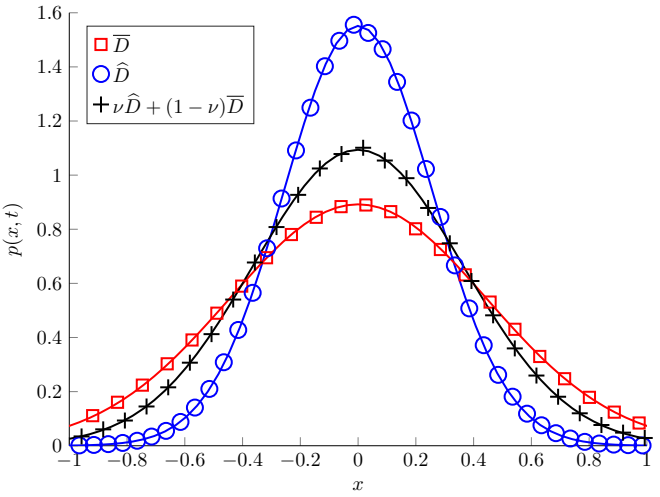

FIG. 1. Convergence of hybrid colored noise process to various SDEs depending on ratio of correlation time to mean switching time for spatially constant switching rates. The red, blue, and black curves are the respective distributions of (2.6), (2.12), and (4.9), which are Gaussians with zero mean and variance $2t\overline{D}$, $2t\widehat{D}$, and $2t[\nu_\eta\widehat{D}+(1-\nu_\eta)\overline{D}]$. The squares, circles, and plusses are the empirical distribution of the hybrid colored noise process (2.4) with mean switching time $\epsilon=10^{-4}$ and respective correlation times $\kappa=\epsilon^2$ ($\eta=10^{-12}$), $\kappa=\epsilon^{1/4}$ ($\eta=10^2$), or $\kappa=\epsilon^{1/2}$ ($\eta=1$) for 10^6 trials. Simulations of the hybrid colored noise process were performed according to the statistically exact algorithm described in Sec. V. The distributions are at time $t=1$ with $D_0=10^{-2}$, $D_1=1$, $\alpha=1-\beta=0.9091$, and thus $\overline{D}=.1$, $\widehat{D}=0.3306\overline{D}$, and $\nu=1/2$.

In Fig. 1, we consider spatially constant switching rates. In this case, the probability distribution of the limiting process, (2.6), (2.12), or (4.9), at time $t>0$ is Gaussian with zero mean and respective variance

$$2t\overline{D},\quad 2t\widehat{D},\quad\text{or}\quad 2t[\nu_\eta\widehat{D}+(1-\nu_\eta)\overline{D}].$$

In addition to verifying that the numerics agree with the theory, Fig. 1 shows that the distributions of the three limiting processes, (2.6), (2.12), and (4.9), can be quite different, even for spatially constant switching rates. Indeed, comparing the formulas for $\overline{D}$ and $\widehat{D}$ in Eqs. (2.7) and (2.11) shows that the ratio $\widehat{D}/\overline{D}$ can be as small as

$$\widehat{D}/\overline{D}=\frac{4\sqrt{D_0/D_1}}{(\sqrt{D_0/D_1}+1)^2}<4\sqrt{D_0/D_1},\tag{5.1}$$

for α,β chosen appropriately. Equation (5.1) shows that the possible discrepancy between the effective diffusion coefficients, $\overline{D}$ and $\widehat{D}$, is related to the discrepancy between the two diffusivities, D_0 and D_1. We therefore note that single-particle tracking experiments have found that antigens diffusing on the surface of T cells can switch between two diffusivities D_0 and D_1 with $D_0/D_1\approx 5\times 10^{-2}$ (see Table 1 in Ref. [23]). In the case of Fig. 1, we take $D_0=10^{-2}<D_1=1$ and $\alpha=1-\beta=0.9091$ so the ratio is $\widehat{D}/\overline{D}=0.3306$.

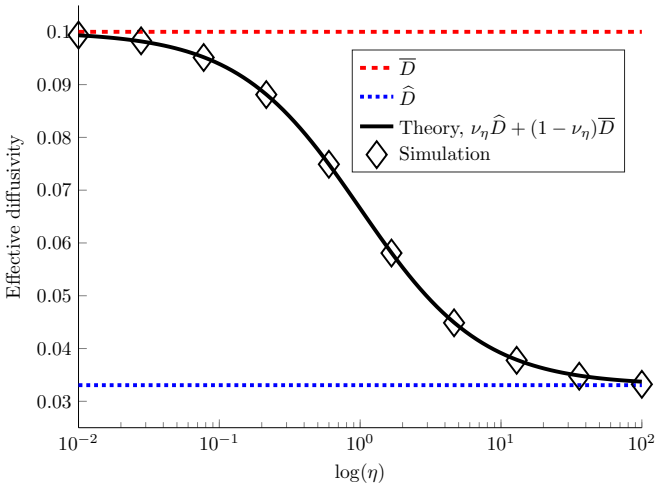

FIG. 2. Effective diffusivity of hybrid colored noise process as a function of ratio of correlation time to mean switching time, $\eta = \kappa^2/\epsilon$, for spatially constant switching rates. The red dashed line is $\overline{D}$ in Eq. (2.7), the blue dotted line is $\widehat{D}$ in Eq. (2.11), and the black solid line is the effective diffusivity, $\nu_\eta \widehat{D} + (1-\nu_\eta)\overline{D}$, with ν_η in Eq. (4.8). The black diamonds are one half of the empirical variance of 10^6 simulations of the hybrid colored noise process until time $t = 1$. The parameters, $\epsilon, \alpha, \beta, D_0, D_1$, are given in the caption of Fig. 1.

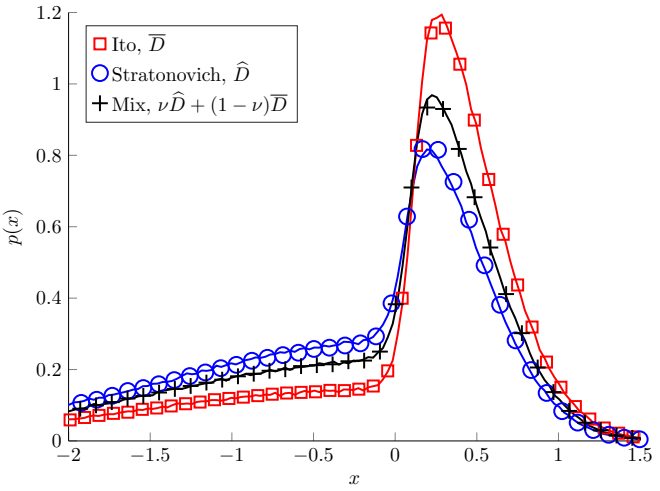

FIG. 3. Convergence of hybrid colored noise process to various SDEs depending on the ratio of correlation time to mean switching time for space-dependent switching rates, $\alpha(x) = \beta(-x) = \tanh(10x) + 1$. The red, blue, and black curves are the respective empirical distributions of (2.6), (2.12), and (4.9), for 10^6 trials. The squares, circles, and plusses are the empirical distribution of the hybrid colored noise process (2.4) with mean switching time $\epsilon = 10^{-3}$ and respective correlation times $\kappa = \epsilon^2$ ($\eta = 10^{-9}$), $\kappa = \epsilon^{1/3}$ ($\eta = 10$), or $\kappa = \epsilon^{1/2}$ ($\eta = 1$) for 10^6 trials. Simulations of (2.12), (2.6), and (4.9) were performed using the Euler-Maruyama method with a discrete time step of size 10^{-3}. Simulations of the hybrid colored noise process were performed according to the statistically exact algorithm described in Sec. V. The distributions are at time $t = 1$ with $D_0 = 10^{-1}$ and $D_1 = 1$.

Figure 2 plots the effective diffusivity of the hybrid colored noise process for a range of ratios of correlation time to mean switching time, $\eta = \kappa^2/\epsilon$, for spatially constant switching rates. In addition to verifying the theory of Secs. III–IV, this figure illustrates that as η varies, there is a sharp transition between the regime in which the effective diffusivity is approximately $\overline{D}$ and the regime in which the effective diffusivity is approximately $\widehat{D}$. Indeed, for the parameters in Fig. 2, the transition essentially occurs between $\eta = 0.1$ and $\eta = 10$.

Moving to space-dependent switching rates, Fig. 3 demonstrates the convergence of (2.4) to either (2.6), (2.12), or (4.9) for

$$\alpha(x) = \beta(-x) = \tanh(10x) + 1.$$

This choice of switching rates makes $X(t)$ more likely to have diffusivity D_0 (respectively, D_1) when $X(t) > 0$ (respectively, $X(t) < 0$); see the top panel of Fig. 4. This models the generic situation in which the diffusing particle is more likely to be in one conformational state when it is one spatial region, perhaps due to spatial heterogeneity of a substrate that binds to the particle and affects its diffusivity. Figure 3 shows that the distributions of the three limiting processes, (2.6), (2.12), and (4.9), are quite different. This discrepancy stems from the different interpretations of the multiplicative noise (Itô versus Stratonovich), in addition to the difference between $\overline{D}(x)$ and $\widehat{D}(x)$, which are actually relatively close in this case; see the bottom panel of Fig. 4.

A. Exact stochastic simulation algorithm

We now describe our stochastic simulation algorithm for drawing statistically exact samples of the three-component hybrid colored noise process $(X(t), Y(t), N(t))$ defined in (2.3) and (2.4). Our algorithm relies on two main ideas. First, we can draw statistically exact samples of $X(t), Y(t)$ away from jump times of $N(t)$ since the FP equation for Ornstein-Uhlenbeck processes can be solved analytically [34]. Second, since the jump rates of $N(t)$ depend on $X(t)$, we draw statistically exact samples of the jump times of $N(t)$ by adapting the classical Poisson thinning method [35,36] for simulating inhomogeneous Poisson processes.

For a given value $[X(s), Y(s), N(s)]$, suppose we want to generate a realization of $[X(s+T), Y(s+T), N(s+T)]$ for some time $T > 0$. The first step is to generate the first possible jump time of $N(t)$ for $t > s$. For simplicity, we assume $\alpha(x), \beta(x)$ are bounded, though one could easily extend to the case where $\alpha(x), \beta(x)$ are only continuous. Let $\lambda > 0$ be such that

$$\sup_x \{\alpha(x), \beta(x)\} < \lambda.$$

We then generate τ_1 according to an exponential distribution with rate λ. If $\tau_1 < T$, then we generate $X(s+\tau_1)$ and $Y(s+\tau_1)$ according to Ref [34]:

$$\begin{aligned} Y(s+\tau_1) &= \mu(\tau_1) Y(s) + \sigma(\tau_1)\xi_1, \\ X(s+\tau_1) &= X(s) + \frac{1}{\kappa}\sqrt{2D_{N(s)}}\{[1-\mu(\tau_1)]\kappa^2 Y(s) \\ &\quad + \sqrt{\theta^2(\tau_1) - [\zeta(\tau_1)/\sigma(\tau_1)]^2}\xi_2 \\ &\quad + [\zeta(\tau_1)/\sigma(\tau_1)]\xi_1\}, \end{aligned} \tag{5.2}$$

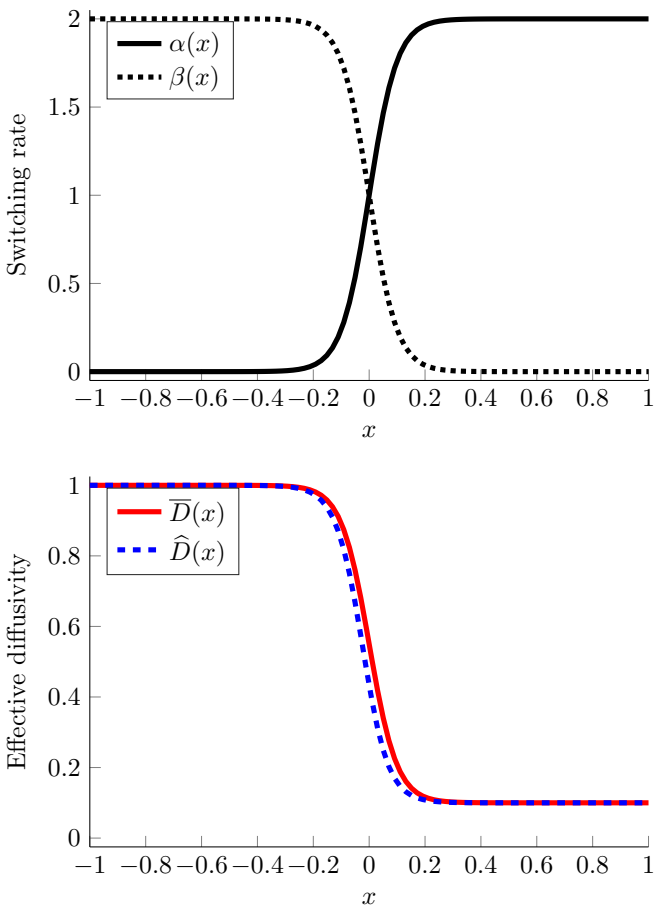

FIG. 4. Top: Space-dependent switching rates, $\alpha(x) = \beta(-x) = \tanh(x) + 1$. Bottom: Effective diffusivity $\overline{D}(x)$ in Eq. (2.7) and effective diffusivity $\widehat{D}(x)$ in Eq. (2.11) for $D_0 = 10^{-1}$, $D_1 = 1$, and $\alpha(x) = \beta(-x) = \tanh(x) + 1$.

where ξ_1, ξ_2 are independent standard normal random variables and

$$\mu(t) := e^{-t/\kappa^2},$$
$$\sigma(t) := \sqrt{\frac{1-\mu(t)^2}{2}},$$
$$\theta(t) := \kappa^2\sqrt{t/\kappa^2 - 2[1-\mu(t)] + [1-\mu(t)^2]/2},$$
$$\zeta(t) := \kappa^2[1-\mu(t)]^2/2.$$

We then set $N(s+\tau_1) = 1 - N(s)$ with probability

$$\frac{N(s)\alpha[X(s+\tau_1)] + [1-N(s)]\beta[X(s+\tau_1)]}{\lambda},$$

and $N(s+\tau_1) = N(s)$ otherwise. With this value of $[X(s+\tau_1), Y(s+\tau_1), N(s+\tau_1)]$, we then generate the next possible jump time, τ_2, of $N(t)$ for $t > s+\tau_1$ according to an exponential distribution with rate λ and repeat this procedure until we reach a point when $\sum_k^K \tau_k > T$. At this point, we generate $X(s+T), Y(s+T)$ according to Eq. (5.2) with the s in Eq. (5.2) replaced by $\sum_k^{K-1} \tau_k$ and the τ_1 in Eq. (5.2) replaced by $T - \sum_k^{K-1} \tau_k$.

VI. DISCUSSION

We have considered a hybrid colored additive noise process in which a particle randomly switches between two diffusivities with mean switching time characterized by a dimensionless parameter $\epsilon > 0$, and whose correlation time is characterized by a dimensionless parameter $\kappa > 0$. In the parameter regime that ϵ and κ are both small, we have found that the effective diffusion process depends on the ratio κ^2/ϵ. In the case that the switching rates depend on the position of the particle, then the effective diffusion is of Itô form if $\kappa^2/\epsilon \ll 1$, Stratonovich form if $\kappa^2/\epsilon \gg 1$, and a mixture of the two if $\kappa^2/\epsilon = O(1)$. Furthermore, even in the case of spatially constant switching rates, the effective diffusion coefficient can vary dramatically depending on κ^2/ϵ.

For simplicity, we have focused on one-dimensional (1D) models with pure diffusion and only two diffusing states. However, it would be possible to extend our analysis to diffusion in two or more space dimensions and any finite number of diffusing states. In particular, in the case of particles switching between N conformational states with distinct diffusivities $D_n, n = 0, 1, \ldots, N-1$, the expressions (2.7) and (2.11) for the effective diffusion coefficients $\overline{D}(x)$ and $\widehat{D}(x)$ still hold, with the sums now taken over $n = 0, 1, \ldots, N-1$. One could also include n-dependent external forcing or drift terms by taking

$$dX(t) = F_{N(t)}[X(t)] + \frac{1}{\kappa}\sqrt{2D_{N(t)}}Y(t)dt, \quad (6.1a)$$
$$dY(t) = -\frac{1}{\kappa^2}Y(t)dt + \frac{1}{\kappa}dW(t). \quad (6.1b)$$

In this case, one finds that the effective drift term in the double limit $\epsilon, \kappa \to 0$ is

$$\overline{F}(X) = \sum_n F_n(X)\rho_n$$

irrespective of the order of the limits, provided that the correct form of the diffusion term is taken.

ACKNOWLEDGMENTS

P.C.B. was supported by the National Science Foundation (DMS-1613048). S.D.L. was supported by the National Science Foundation (DMS-RTG 1148230).

[1] R. Mannella and P. V. E. McClintock, Fluct. Noise Lett. **11**, 1240010 (2012).
[2] P. F. Tupper and X. Yang, Proc. R. Soc. A **468**, 3864 (2012).
[3] T. Kuroiwa and K. Miyazak, J. Phys. A **47**, 012001 (2014).
[4] C. W. Gardiner, *Handbook of Stochastic Methods*, 4th ed. (Springer, Berlin, 2009).
[5] Y. L. Klimontovich, Phys. A (Amsterdam, Neth.) **163**, 515 (1990).

[6] A. W. C. Lau and T. C. Lubensky, Phys. Rev. E **76**, 011123 (2007).
[7] P. Ao, C. Kwon, and H. Qian, Complexity **12**, 19 (2007).
[8] G. Volpe, L. Helden, T. Brettschneider, J. Wehr, and C. Bechinger, Phys. Rev. Lett. **104**, 170602 (2010).
[9] P. Lançon, G. Batrouni, L. Lobry, and N. Ostrowsky, Europhys. Lett. **54**, 28 (2001).
[10] T. Brettschneider, G. Volpe, L. Helden, J. Wehr, and C. Bechinger, Phys. Rev. E **83**, 041113 (2011).
[11] H. Qian, M. P. Sheetz, and E. L. Elson, Biophys. J. **60**, 910 (1991).
[12] M. J. Saxton and K. Jacobson, Ann. Rev. Biophys. Biomol. Struct. **26**, 373 (1997).
[13] A. Kusumi, C. Nakada, K. Ritchie, K. Murase, K. Suzuki, H. Murakoshi *et al.*, Ann. Rev. Biophys. Biomol. Struct. **34**, 351 (2005).
[14] A. Kusumi, K. G. N. Suzuki, R. S. Kasai, K. Ritchieand, T. K. Fujiwara, Trends Biochem. Sci. **36**, 604 (2011).
[15] C. Eggeling, C. Ringemann, R. Medda, G. Schwarzmann, K. Sandhoff, S. Polyakova *et al.*, Nature (London) **457**, 1159 (2009).
[16] C. W. Cairo, R. Mirchev, and D. E. Golan, Immunity **25**, 297 (2006).
[17] P. Massignan, C. Manzo, J. A. Torreno-Pina, M. F. García-Parajo, M. Lewenstein, and G. J. Lapeyre, Jr., Phys. Rev. Lett. **112**, 150603 (2014).
[18] C. Manzo, J. A. Torreno-Pina, P. Massignan, G. J. Lapeyre, Jr., M. Lewenstein, and M. F. Garcia Parajo, Phys. Rev. X **5**, 011021 (2015).
[19] J. Meier, C. Vannier, A. Sergé, A. Triller, and D. Choquet, Nat. Neurosc. **4**, 253 (2001).
[20] S. Huet, E. Karatekin, V. S. Tran, I. Fanget, S. Cribier, and J.-P. Henry, Biophys. J. **91**, 3542 (2006).
[21] N. Meilhac, L. Le Guyader, L. Salomé, and N. Destainville, Phys. Rev. E **73**, 011915 (2006).
[22] V. Rajani, G. Carrero, D. E. Golan, G. de Vries, and C. W. Cairo, Biophys. J. **100**, 1463 (2011).
[23] R. Das, C. W. Cairo and D. Coombs, PLoS Comp. Biol. **5**, e1000556 (2009).
[24] F. Persson, M. Lindén, C. Unoson, and J. Elf, Nat. Meth. **10**, 265 (2013).
[25] P. J. Slator, C. W. Cairo, and N. J. Burroughs, PLoS ONE **10**, e0140759 (2015).
[26] E. Yamamoto, T. Akimotot, A. C. Kalli, K. Yasuoka, and M. S. P. Sansom, Sci. Adv. **3**, e1601871 (2017).
[27] P. C. Bressloff and S. D. Lawley, Phys. Rev. E **95**, 060101(R) (2017).
[28] A. Godec and R. Metzler, J. Phys. A **50**, 084001 (2017).
[29] P. C. Bressloff, Phys. Rev. E **94**, 042129 (2016).
[30] G. C. Papanicolaou, Bull. Amer. Math. Soc. **81**, 330 (1975).
[31] J. Newby and P. C. Bressloff, Bull. Math. Biol. **72**, 1840 (2010).
[32] G. A. Pavliotis, *Stochastic Processes and Applications* (Springer, New York, 2014).
[33] A. G. Ramm, Am. Math. Mon. **108**, 855 (2001).
[34] D. T. Gillespie, Phys. Rev. E **54**, 2084 (1996).
[35] P. A. W Lewis and G. S. Shedler, Nav. Res. Logist. Q. **26**, 403 (1979).
[36] S. M. Ross, *Simulation*, 2nd ed. (Academic Press, San Diego, 1997).